

1 **EVANESCENT ACOUSTIC-GRAVITY MODES IN THE ISOTHERMAL**
2 **ATMOSPHERE: SYSTEMATIZATION, APPLICATIONS TO THE EARTH'S**
3 **AND SOLAR ATMOSPHERES**

4
5 **Oleg K. Cheremnykh, Alla K. Fedorenko, Evgen I. Kryuchkov, Yuriy A. Selivanov**

6
7 Space Research Institute NASU-SSAU, Kyiv, 03187, Ukraine

8 *Correspondence to:* Yuriy A. Selivanov (yuraslv@gmail.com)

9
10 **Abstract.** The objects of research in this work are evanescent wave modes in a gravitationally
11 stratified atmosphere and their associated pseudo-modes. Whereas the former, according to the
12 dispersion relation, rapidly decrease with distance from a certain surface, the latter, having the same
13 dispersion law, differ from the first by the form of polarization and the nature of decreasing from the
14 surface. Within a linear hydrodynamic model, the propagation features of evanescent wave modes in
15 an isothermal atmosphere are studied. Research carried out for different assumptions about the
16 properties of the disturbances. On this way, a new wave mode - anelastic evanescent wave mode -
17 was discovered that satisfies the dispersion relation $\omega^2 = k_x g (\gamma - 1)$. Also, the possibility of the
18 existence of a pseudo-mode related to it is indicated. The case of two isothermal media differing in
19 temperature at the interface is studied in detail. It is shown that a non-divergent pseudo-mode with a
20 horizontal scale $k_x \sim 1/2H_1$ can be realized on the interface with dispersion $\omega^2 = k_x g$. Dispersion
21 relation $\omega^2 = k_x g (\gamma - 1)$ at the interface of two media is satisfied by the wave mode, which has
22 different types of amplitude versus height dependencies at different horizontal scales k_x . The
23 applicability of the obtained results to clarify the properties of f -mode observed on the Sun is
24 analyzed.

25
26 **Keywords:** acoustic-gravity waves, evanescent wave modes, isothermal atmosphere, solar
27 atmosphere, earth's atmosphere

28
29 **1 Introduction**

31 Acoustic - gravity waves (AGWs) in the Earth's atmosphere are studied theoretically and
32 experimentally for more than 60 years. The linear theory of AGW (Hines, 1960; Yeh and Liu,
33 1974; Francis, 1975) admits the existence in the atmosphere of a continuous spectrum of freely
34 propagating waves, consisting of acoustic and gravity regions on the dispersion plane, as well as of
35 evanescent modes, which can only propagate horizontally.

36 The freely propagating AGWs effectively transfer the energy and momentum between various
37 atmospheric layers and thus play an important role in the dynamics and energy balance of the
38 atmosphere. These waves are generated by various sources (both natural and technogenic ones),
39 which are accompanied by a significant energy output into the atmosphere. Further, when the
40 AGWs propagate upward the energy conservation compensates for the decrease of the atmospheric
41 density with the height by exponentially increasing amplitude. Therefore at a certain height the
42 waves become nonlinear. Significant progress in the development of the nonlinear theory of AGW
43 was achieved by a number of authors, in particular, Belashov (1990), Nekrasov et al. (1995),
44 Kaladze et al. (2008), Stenflo and Shukla (2009), Huang et al. (2014). Numerical modeling of the
45 freely propagating AGWs in the realistic viscous and heat-conducting atmosphere is an important
46 area of modern studies of these waves (i.e. Vadas, 2012; Cheremnykh et al., 2010).

47 Satellite observations of AGWs in the Earth's polar thermosphere indicate a prevailing presence
48 of waves with oscillation periods concentrated around the Brunt-Väisälä period and of horizontal
49 scale of about 500 - 700 km (Johnson et al., 1995; Innis and Conde, 2002; Fedorenko et al.,
50 2015). Azimuths of the propagation of these AGW demonstrate the close connection with the
51 directions of background winds in the thermosphere. Moreover, the amplitudes of the waves depend
52 on the speed of headwind but do not depend on height (Fedorenko and Kryuchkov, 2013;
53 Fedorenko et al., 2018). These experimental results cannot be sufficiently explained by the theory of
54 freely propagating AGWs. They may indicate waveguide or evanescent (along a horizontal surface)
55 propagation of at least part of the observed waves.

56 As well as freely propagating AGWs, evanescent wave modes also play an important role in
57 atmospheric dynamics of the Sun and planets. Evanescent waves propagate horizontally in an
58 atmosphere, vertically stratified by gravity, subject to the presence of vertical gradients of
59 parameters. The energy of these waves should decrease both up and down from the level at which
60 they are generated. Therefore, evanescent waves are most effectively generated in areas of presence
61 of significant vertical gradients of temperature and density or strong local currents. For example, in
62 the solar atmosphere suitable conditions for realization evanescent modes occur at the boundary

63 between the chromosphere and corona (Jones, 1969). In the Earth's atmosphere, such waves can be
 64 efficiently generated at sharp vertical temperature gradients, for example, at the base of the
 65 thermosphere or at the heights of the tropo- and mesopause. Also, evanescent wave modes can
 66 emerge in the presence of strong inhomogeneous winds, for example, in the region of the polar
 67 circulation of the thermosphere.

68 The study of evanescent waves traditionally gets less attention than the study of freely
 69 propagating AGWs. The most known of them are the horizontal Lamb wave and vertical oscillations
 70 with Brunt–Väisälä (BV) frequency (Beer, 1974; Waltercheid and Hecht, 2003). In hydrodynamics,
 71 physics of terrestrial and solar atmosphere, the surface gravity mode with dispersion $\omega^2 = k_x g$ is
 72 also well studied (Tolstoy, 1963; Jones, 1969). In particular, it was shown that it is the fundamental
 73 mode (f - mode) of oscillations in the solar atmosphere (Jones, 1969). Experimental f - mode
 74 observations are used to study flows, refinement of the solar radius and other parameters of the Sun
 75 (Ghosh et al., 1995; Antia, 1998). In the earth's atmosphere, evanescent waves are often observed at
 76 altitudes near the mesopause using ground-based instrumentation (Shimkhada et al., 2009).

77 In this paper, different types of evanescent acoustic-gravity modes characteristic of an
 78 isothermal atmosphere are investigated using a set of linearized hydrodynamic equations. In
 79 particular, the possibility of the existence of a new type of evanescent acoustic-gravity modes with
 80 the dispersion $\omega^2 = k_x g(\gamma - 1)$ is proved in the assumption of anelasticity of the disturbance. Also
 81 the possibility of realization the evanescent modes in the model of a thin temperature gap studied.

82

83 2 Evanescent modes in the isothermal atmosphere

84

85 Consider an unbounded ideal isothermal atmosphere, stratified in a field of gravity. Linear
 86 perturbations in such a medium satisfy a set of four first order hydrodynamic equations (Hines,
 87 1960). These equations are convenient to bring to a set of two second order equations for the
 88 perturbations of the horizontal V_x and vertical V_z particle velocities (Tolstoy, 1963):

$$89 \quad \rho_0 \frac{\partial^2 V_x}{\partial t^2} = -\rho_0 g \frac{\partial V_z}{\partial x} + \frac{\partial}{\partial x} \left[\rho_0 c^2 \left(\frac{\partial V_x}{\partial x} + \frac{\partial V_z}{\partial z} \right) \right], \quad (1)$$

$$90 \quad \rho_0 \frac{\partial^2 V_z}{\partial t^2} = \rho_0 g \frac{\partial V_x}{\partial z} + \frac{\partial}{\partial z} \left[\rho_0 c^2 \left(\frac{\partial V_x}{\partial x} + \frac{\partial V_z}{\partial z} \right) \right], \quad (2)$$

91 where ρ_0 , γ , g denote background atmosphere density, ratio of specific heats, acceleration of
 92 gravity, respectively; $c = \sqrt{\gamma g H}$ is the sound speed, $H = -\rho_0 / (d\rho_0 / dz) = kT / mg$ is the density
 93 scale height, T is the temperature, k is the Boltzmann constant, m is the molecular mass of the
 94 atmospheric gas.

95 Solutions to the system (1), (2) are usually searched for in the form:

$$96 \quad V_x, V_z \sim \exp(az) \exp[i(\omega t - k_x x)] , \quad (3)$$

97 where ω , k_x are cyclic frequency and horizontal component of the wave vector, respectively;
 98 parameter a sets the vertical scale of the change in the amplitude of velocities, V_x and V_z , with the
 99 height, z . For brevity, we will refer to a as the stratification of the corresponding mode.

100 The system (1), (2) allows, on the plot “frequency-wave number”, for the existence of gravity
 101 and acoustic regions of freely propagating waves, for which $a = \frac{1}{2H} \pm ik_z$ (Hines, 1960), where k_z
 102 is the vertical component of the wave vector. Also, from (1), (2) we get the solutions in the form of
 103 evanescent wave modes having real a and propagating horizontally (Waltercheid and Hecht,
 104 2003). Solutions in the form of evanescent modes are usually obtained by imposing additional
 105 conditions on the perturbation properties.

106

107 **2.1 Non - divergent and pseudo - non - divergent modes**

108

109 Let us note the well known in hydrodynamics approximation of perturbations incompressibility (see,
 110 e.g., Ladikov-Roev et al., 2010), for which

$$111 \quad \text{div} \vec{V} = \frac{\partial V_x}{\partial x} + \frac{\partial V_z}{\partial z} = 0 . \quad (4)$$

112 In frames of this approximation, we obtain the following equations from (1), (2):

$$113 \quad \frac{\partial^2 V_x}{\partial t^2} = -g \frac{\partial V_z}{\partial x} , \quad (5)$$

$$114 \quad \frac{\partial^2 V_z}{\partial t^2} = g \frac{\partial V_x}{\partial x} . \quad (6)$$

115 After substituting (3) into equations (5), (6) we find:

$$116 \quad -\omega^2 V_x = ik_x g V_z ,$$

117 $-\omega^2 V_z = -ik_x g V_x .$

118 This yields a dispersion equation for incompressible wave modes in the form

119 $\omega^2 = k_x g .$ (7)

120 Given the dispersion found, we obtain an expression for the polarization of the incompressible
121 modes:

122 $V_z = iV_x .$ (8)

123 Further, from the condition (4) and polarization (8) we get $a = k_x$. Insofar as a is real value then
124 non - divergent (ND) wave mode has no periodic vertical solution and is horizontally propagating.

125 Let us show that the dispersion relation (7) is also satisfied by another wave mode. After using
126 this relation in (1), (2) we get:

127 $V_x (\gamma H k_x - 1) - iV_z (1 - \gamma a H) = 0 ,$ (9)

128 $iV_x (1 - \gamma H a - \gamma) - V_z \left(1 + \frac{\gamma H a^2}{k_x} - \frac{\gamma a}{k_x} \right) = 0 .$ (10)

129 From the system (9), (10) follows:

130 $a^2 - \frac{a}{H} + \frac{k_x}{H} (1 - k_x H) = 0 ,$

131 which implies that there are two solutions to this equation:

132 $a = k_x , a = \frac{1}{H} - k_x .$ (11)

133 The first solution in (11) corresponds to the non-divergent (ND) wave mode, and the second
134 one we call pseudo-non-divergent mode (NDp). The expression for polarization NDp is obtained
135 from (9) and has the form:

136 $V_x \left(\frac{1}{\gamma H} - k_x \right) = -i \left(k_x - \frac{\gamma - 1}{\gamma H} \right) V_z .$

137 Also for this mode holds the equation

138 $div \vec{V} = \frac{V_z}{H} \frac{(1 - 2k_x H)}{(1 - \gamma k_x H)} ,$

139 which shows that for NDp mode $div \vec{V} = 0$ only when $k_x = 1/2H$.

140

141 **2.2 Anelastic and pseudo-anelastic modes**

142

143 Let us show that equations (1), (2) indicate that another wave mode, not previously studied, may
 144 exist. To do this, we introduce, according to Bannon (1996), the anelastic linear perturbations, which
 145 satisfy the condition

146
$$\operatorname{div}(\rho_0 \vec{V}) = 0 . \quad (12)$$

147 In the isothermal atmosphere with barometric density distribution we have

148
$$\frac{\partial \rho_0}{\partial z} = -\frac{\rho_0}{H} ,$$

149 therefore, for such *anelastic* perturbations, the following equation holds:

150
$$\operatorname{div} \vec{V} = \frac{V_z}{H} . \quad (13)$$

151 Substituting (13) into equations (1), (2) we get:

152
$$\frac{\partial^2 V_x}{\partial t^2} = g(\gamma - 1) \frac{\partial V_z}{\partial x} ,$$

153
$$\frac{\partial^2 V_z}{\partial t^2} = -g(\gamma - 1) \frac{\partial V_x}{\partial x} .$$

154 Thus, given (3), should:

155
$$\omega^2 V_x = ik_x g(\gamma - 1) V_z , \quad (14)$$

156
$$\omega^2 V_z = -ik_x (\gamma - 1) g V_x . \quad (15)$$

157 Then the dispersion equation for *anelastic* (AE) *modes* takes the form:

158
$$\omega^2 = k_x g(\gamma - 1). \quad (16)$$

159 With the resulting dispersion, polarization follows from equations (14), (15):

160
$$V_x = iV_z . \quad (17)$$

161 Further, taking into account (13), we obtain $a = \frac{1}{H} - k_x$. Consequently, the AE mode also does not
 162 have a solution periodic vertically and can only propagate horizontally.

163 After substituting the dispersion (16) into equations (1), (2) we get:

164
$$V_x (1 - \gamma + \gamma H k_x) - iV_z (1 - \gamma a H) = 0 , \quad (18)$$

$$165 \quad iV_x(1-\gamma+\gamma Ha)+V_z\left(1-\gamma-\frac{\gamma Ha^2}{k_x}+\frac{\gamma a}{k_x}\right)=0, \quad (19)$$

166 whence we get a pair of values a , identical to (11). Consequently, there is another wave solution
 167 that satisfies the equation (16), we call it *pseudo-anelastic (AEp) mode*. The first value in (11)
 168 corresponds to the AEp wave mode, and the second – to the AE one.

169 Polarization of the AEp mode has the form:

$$170 \quad V_x\left(k_x-\frac{\gamma-1}{\gamma H}\right)=-i\left(\frac{1}{\gamma H}-k_x\right)V_z$$

171 that follows from (18) or (19).

172

173 3 General properties of evanescent modes

174

175 Let us prove that the different types of evanescent modes characteristic of an isothermal atmosphere
 176 are related. We substitute (3) into system (1), (2) without additional conditions that were imposed in
 177 Section 2 when deriving ND and AE mode. As a result, we get:

$$178 \quad V_z\left(a-\frac{g}{c^2}\right)-ik_xV_x\left(1-\frac{\omega^2}{k_x^2c^2}\right)=0, \quad (20)$$

$$179 \quad V_x\left(a-\frac{N^2}{g}\right)-ik_xV_z\left(\frac{N^2}{\omega^2}-1\right)=0, \quad (21)$$

180 where $N^2 = \frac{g}{H} \frac{(\gamma-1)}{\gamma}$ is the square of the Brunt-Väisälä frequency.

181 From system (20), (21) we obtain the dispersion equation:

$$182 \quad \left(\frac{1}{\gamma H}-a\right)\left(a-\frac{\gamma-1}{\gamma H}\right)=k_x^2\left(\frac{N^2}{\omega^2}-1\right)\left(1-\frac{\omega^2}{k_x^2c^2}\right). \quad (22)$$

183 Expressions $\omega^2 = N^2$ and $\omega^2 = k_x^2c^2$ are well-known dispersions of Brunt-Väisälä
 184 oscillations with $a = 1/\gamma H$ and Lamb waves (L) with $a = (\gamma-1)/\gamma H$. In addition to these known
 185 modes, dispersion (22) also admits the existence of additional solutions in the form of BV pseudo-
 186 modes (BVp) with $\omega^2 = N^2$, $a = (\gamma-1)/\gamma H$ and Lamb pseudo-modes (Lp) with $\omega^2 = k_x^2c^2$,
 187 $a = 1/\gamma H$ (Beer, 1974; Waltercheid and Hecht, 2003).

188 Then represent (22) in the form of a quadratic equation with respect to a :

$$189 \quad a^2 - \frac{a}{H} + \frac{\omega^2}{c^2} - k_x^2 + \frac{k_x^2 g^2}{\omega^2 c^2} (\gamma - 1) = 0 .$$

190 The solution to this equation is:

$$191 \quad a = \frac{1}{2H} \pm \sqrt{\frac{(k_x g - \omega^2)(\omega^2 - k_x g(\gamma - 1))}{\omega^2 c^2} + \left(k_x - \frac{1}{2H}\right)^2} . \quad (23)$$

192 From which it follows that for modes with dispersions $\omega^2 = k_x g(\gamma - 1)$ and $\omega^2 = k_x g$ there are two
 193 possible values: $a = k_x$ and $a = \frac{1}{H} - k_x$. The first value corresponds to modes ND and AEp, and the
 194 second - NDp and AE.

195 Thus, each evanescent mode can be associated with a pseudo-mode, which satisfies the same
 196 dispersion relation, but differs in polarization and dependence of the amplitude from the height, i.e.,
 197 in its stratification. Table 1 presents the properties of different evanescent modes, characteristic of
 198 the isothermal atmosphere: BV oscillations, Lamb waves, non-divergent and anelastic modes, along
 199 with associated pseudo-modes: BVp, Lp, NDp, AEp. Table 1 shows that for all pseudo-modes, the
 200 polarization changes depending on the value of k_x . Wave modes AE and ND at $k_x = 1/2H$
 201 completely coincide with AEp and NDp, respectively.

202 The location of the dispersion curves for anelastic and non-divergent modes relative to gravity
 203 and acoustic regions in the (ω, k_x) plane is shown in Fig. 1. The $\omega^2 = k_x g(\gamma - 1)$ mode touches the
 204 gravity region of freely propagating AGWs at the same value $k_x = 1/2H$ at which the $\omega^2 = k_x g$
 205 curve touches the acoustic region (see Figure 1). In this case, the dispersion curves of AE and ND
 206 modes are symmetric relative to the ‘‘characteristic’’ curve (see Beer, 1974), which separates the
 207 AGW acoustic region from the AGW gravity region. In fact, the characteristic curve is the
 208 geometric mean of the dispersion curves of AE and ND modes with $\omega^2 = \sqrt{k_x^2 g^2 (\gamma - 1)} = N k_x c$.

209 From Figure 1 we see that the dispersion curves of different evanescent modes have intersection
 210 at separate points. Lamb dispersion curve with $\omega^2 = k_x^2 c^2$ intersects with BV curve with
 211 $\omega^2 = N^2$ at the point $k_x = N/c$. However, these modes cannot interact with each other by reason
 212 of different polarizations and values of a . At the same time, the pairs Lp - BV and L - BVp
 213 completely coincide in these properties and are indistinguishable at the intersection points.

214 Dispersion curves $\omega^2 = k_x g$ and $\omega^2 = k_x g(\gamma - 1)$ intersect with the Lamb curve and the BV
215 curve at points $k_x = 1/\gamma H$, $k_x = (\gamma - 1)/\gamma H$. In addition, the ND mode curve intersects with the
216 Lamb curve at the same value k_x , at which the AE mode curve intersects with the BV curve (see
217 Fig. 1). ND and AE modes cannot interact with the Lamb mode and BV oscillations due to different
218 polarizations (Table 1). Pseudo-modes NDp and AEp, at the points of intersection with the Lamb
219 wave and the BV oscillations, have the same polarization and values of a . Similarly, ND and AE
220 are indistinguishable at the points of intersection with Lp and BVp. Table 2 shows all evanescent
221 modes that coincide with each other at the points of intersection of the dispersion curves, and
222 between which interaction is possible. The cases of ND and AE mode curves intersection with
223 curves ($a = 1/2H$), which separate the area of freely propagating AGWs from the evanescent
224 area, are not presented in Table 2.

225

226 **4 The energy of evanescent modes in an isothermal atmosphere**

227

228 In Sections 2 and 3, we considered a model of an unbounded isothermal stratified atmosphere to
229 determine which types of evanescent modes can satisfy the initial system of equations (1), (2).
230 However, in an infinitely extended medium, the necessary condition for the existence of evanescent
231 modes is the absence of unlimited growth of oscillation energy above and below the height level at
232 which they are generated. It is easy to verify that in an isothermal infinite atmosphere, none of the
233 modes listed in Table 1 satisfy this condition.

234 Suppose further that an evanescent wave is generated at a certain altitude level $z = 0$. The
235 kinetic energy density $E \sim \rho(z)(V_x^2 + V_z^2)$ of waves should decrease both up and down from the level
236 $z = 0$. When $z \rightarrow +\infty$ the energy density $E \sim \exp\left(2a - \frac{1}{H}\right)z \rightarrow 0$, if $a < 1/2H$, and $E \rightarrow \infty$, if a
237 $a > 1/2H$. When $z \rightarrow -\infty$ the energy density $E \rightarrow 0$, if a $a > 1/2H$ and $E \rightarrow \infty$, if a
238 $a < 1/2H$. Based on these considerations, it is not difficult to understand how the energy density
239 varies with height for different types of evanescent modes in an infinite isothermal atmosphere (see
240 Table 3). Therefore, for the realization of such modes, it is necessary to have boundaries in the
241 medium at which the condition for reducing energy in both directions from this boundary can be
242 satisfied.

243 The presence of boundaries is not the only condition that can limit the energy of the evanescent
 244 mode. If the equality $a = 1/2H$ holds for these modes, then their energy is not varies with height in
 245 an isothermal atmosphere. For an infinite atmosphere, this solution does not seem to be physical,
 246 but it can make sense for a real atmosphere of finite height. As follows from (11), for the ND and
 247 AE modes, as well as their pseudo-modes, the condition $a = 1/2H$ performed at the point
 248 $k_x = 1/2H$. Also, at this point, the ND mode is identical to the NDp mode, and the AE mode
 249 completely coincides with AEp. In addition, when $k_x = 1/2H$ these evanescent modes adjoin the
 250 border of regions of freely propagating AGW (see Fig.1).

251 Consider some features of the energy balance for the evanescent modes. It follows from
 252 equation (20) that:

$$253 \quad |V_z|^2 \left(a - \frac{g}{c^2} \right)^2 = k_x^2 |V_x|^2 \left(1 - \frac{\omega^2}{k_x^2 c^2} \right)^2. \quad (24)$$

254 Combining equations (22) and (24) gives the relation:

$$255 \quad \rho_0 |V_x|^2 \left(1 - \frac{\omega^2}{k_x^2 c^2} \right) \left(a - \frac{N^2}{g} \right) = \rho_0 |V_z|^2 \left(\frac{N^2}{\omega^2} - 1 \right) \left(\frac{g}{c^2} - a \right). \quad (25)$$

256 The average density of the kinetic energy of the perturbations is $E_k = \frac{1}{4} \rho_0 (V_x^2 + V_z^2)$ and of the
 257 potential energy is $E_p = \frac{1}{4} \rho_0 \left(V_x^2 \frac{\omega^2}{k_x^2 c^2} + V_z^2 \frac{N^2}{\omega^2} \right)$ (Yeh, Liu, 1974; Fedorenko, 2010). Therefore,
 258 from equation (25) it follows that for the evanescent modes $E_k \neq E_p$. At the same time, for freely
 259 propagating AGWs is always fulfilled the equality $E_k = E_p$ (Yeh, Liu, 1974). At the point
 260 $a = 1/2H$ where evanescent modes on the plane (ω, k_x) in Fig. 1 are adjacent to areas of freely
 261 propagating AGWs, the equality $a - \frac{N^2}{g} = \frac{g}{c^2} - a$ holds. Taking this circumstance into account,
 262 from (25) we obtain:

$$263 \quad \frac{\rho_0}{4} (|V_x|^2 + |V_z|^2) = \frac{\rho_0}{4} \left(|V_x|^2 \frac{\omega^2}{k_x^2 c^2} + |V_z|^2 \frac{N^2}{\omega^2} \right), \quad (26)$$

264 that is, at this point $E_k = E_p$.

265

266

267 **5 Evanescent modes at the interface of isothermal media**

268

269 Let us consider the possibility of realization of evanescent modes in the atmosphere at a thin
 270 interface between two isothermal half-spaces of infinite extent, which differ in temperature T . Let
 271 the boundary be localized at some altitude level $z=0$. In the lower half-space ($z < 0$) we have
 272 $T = T_1$, while in the upper half-space ($z > 0$) we have $T = T_2$ and it is assumed that $T_2 > T_1$. Note
 273 that a similar model was considered by Rosental and Gough (1994). We will search for solutions to
 274 the system (1), (2) in the form of $V_x, V_z \sim \exp(a_1 z) \exp[i(\omega t - k_x x)]$ for the lower half-plane and in the
 275 form $V_x, V_z \sim \exp(a_2 z) \exp[i(\omega t - k_x x)]$ for the upper half-plane. Substituting these dependencies
 276 into (1), (2) yields:

277
$$a_1 = \frac{1}{2H_1} \pm \left(\frac{1}{4H_1^2} - \frac{\omega^2}{c_1^2} + k_x^2 - k_x^2 \frac{N_1^2}{\omega^2} \right)^{1/2}, \quad (27)$$

278
$$a_2 = \frac{1}{2H_2} \pm \left(\frac{1}{4H_2^2} - \frac{\omega^2}{c_2^2} + k_x^2 - k_x^2 \frac{N_2^2}{\omega^2} \right)^{1/2}. \quad (28)$$

279 Here indices 1 and 2 denote the values in the lower and upper half-spaces, respectively.

280 The density of the kinetic energy of evanescent waves should decrease from the level $z=0$
 281 both up and down. This condition limits the possible values of a_1 and a_2 . In the upper half-space
 282 ($z > 0$), when $z \rightarrow +\infty$ the energy density $E_2 \sim \exp\left(2a_2 - \frac{1}{H_2}\right)z \rightarrow 0$, if $a_2 < 1/2H_2$. In the
 283 lower half-space ($z < 0$), when $z \rightarrow -\infty$ the energy density $E_1 \sim \exp\left(2a_1 - \frac{1}{H_1}\right)z \rightarrow 0$, if
 284 $a_1 > 1/2H_1$. Therefore, it is necessary to take in the expression (27) for a_1 the solution with a “+”
 285 sign and in expression (28) for a_2 , with a “-” sign, so that the energy decreases on both sides of the
 286 interface.

287 It is also necessary to consider that the possible values of a_1 and a_2 must satisfy the boundary
 288 condition (Tolstoy, 1963; Rosental and Gough, 1994), arising from (1), (2):

289

290
$$\rho_1 c_1^2 \frac{gk_x^2 - \omega^2 a_1}{\omega^2 - c_1^2 k_x^2} \Big|_{z=0} = \rho_2 c_2^2 \frac{gk_x^2 - \omega^2 a_2}{\omega^2 - c_2^2 k_x^2} \Big|_{z=0}, \quad (29)$$

291 where ρ_1 and ρ_2 are the densities on both sides of the boundary. The procedure for deriving
 292 equality (29) is exactly the same as in the papers by Cheremnykh et al. (2018a) and Cheremnykh et
 293 al. (2018b). When obtaining (29) we require continuity of the vertical velocity component
 294 (kinematic condition) and perturbed pressure (dynamic condition). In the barometric atmosphere we
 295 have $\rho c^2 = \gamma p_0$, where p_0 is the equilibrium pressure, which must be continuous across the
 296 interface. Therefore, when $\gamma_1 = \gamma_2$ equation (29) can be written as:

$$297 \quad \frac{gk_x^2 - \omega^2 a_1}{\omega^2 - c_1^2 k_x^2} = \frac{gk_x^2 - \omega^2 a_2}{\omega^2 - c_2^2 k_x^2} . \quad (30)$$

298 Dispersion dependencies of $\omega = f(k_x)$ calculated numerically by means of the expression (30)
 299 are shown in Fig. 2a for different values of the parameter $d = H_2 / H_1$. On each of these curves, the
 300 condition for decreasing energy up and down from the interface is satisfied. The long-wavelength
 301 part of the spectrum, where the most interesting features appear, is shown in more detail in Fig. 2b.
 302 Also shown in these figures are the dispersion curves $\omega = \sqrt{k_x g}$ and $\omega = \sqrt{k_x g(\gamma - 1)}$ for the ND
 303 and AE wave modes. The discontinuities of the $\omega = f(k_x)$ curves, as well as their cut-off for
 304 smaller k_x values, are due to requirements $a_1 > 1/2H_1$ and $a_2 < 1/2H_2$. Some features of the
 305 behavior of $\omega = f(k_x)$ will be discussed below.

306 As shown by Miles and Roberts (1992), the dispersion equation (30) can be rewritten to a
 307 polynomial form suitable for analysis:

$$308 \quad \omega^8 - 2c_1^2(d+1)k_x^2\omega^6 + [c_1^4(d+1)^2k_x^4 + (2\gamma-1)k_x^2g^2]\omega^4 - 2(\gamma-1)c_1^2(d+1)k_x^4g^2\omega^2 - c_1^4(d-1)^2k_x^6g^2 = 0$$

$$309 \quad . \quad (31)$$

310 Non-physical solutions (Miles and Roberts, 1992) arising from quadratic expressions under the
 311 radicals were excluded from consideration while obtaining equation (31) (see (27), (28)).
 312 Expressions (31) can be analyzed by examining their asymptotic behavior.

313 If $k_x^2 c_1^2 \gg \omega^2$, then from (31) we get:

$$314 \quad \omega^4 - \frac{2N_1^2}{d+1}\omega^2 - \frac{(d-1)^2}{(d+1)^2}k_x^2g^2 \approx 0 .$$

315 It follows from this expression:

$$316 \quad \omega^2 = \frac{1}{d+1} \left[N_1^2 + \sqrt{N_1^4 + (d-1)^2 k_x^2 g^2} \right]. \quad (32)$$

317 The expression (32) contains an interesting dependence of the frequency on the parameter d . In the
 318 limit $d \rightarrow \infty$, the dispersion $\omega^2 \approx k_x g$ of the ND (NDp) mode, independent of the properties of
 319 both environments, follows from (32). With $d \rightarrow 1$ and using (32), we obtain the dispersion of the
 320 BV (BVp) mode with the parameters of the lower medium, that is, $\omega^2 \approx N_1^2$. The indicated
 321 asymptotic features are visible on the curves shown in Fig. 2 below.

322 In the long-wave limit, i.e., at $k_x \rightarrow 0$, from (31) it follows:

$$323 \quad (2\gamma - 1)\omega^4 - 2(\gamma - 1)c_1^2(d+1)k_x^2\omega^2 - c_1^4(d-1)^2 k_x^4 \approx 0.$$

324 Hence we find:

$$325 \quad \omega^2 = \frac{c_1^2 k_x^2}{2\gamma - 1} \left[(\gamma - 1)(d+1) + \sqrt{\gamma^2(d+1)^2 - 4d(2\gamma - 1)} \right]. \quad (33)$$

326 For the considered small k_x , for different values of d , from (33) we obtain the family of Lamb-
 327 type acoustic modes (see Fig. 2b). For large values of d , using (33), we obtain the expression
 328 $\omega^2 \approx c_1^2 k_x^2 d = c_2^2 k_x^2$, i.e. the oscillation frequency is determined by the characteristics of the medium
 329 in the upper half-space.

330 The evanescent modes frequencies lie on the (ω, k_x) plane between the acoustic and gravity
 331 regions of freely propagating AGW determined for upper and lower media separately (see Fig. 1). It
 332 is necessary to take into account when considering evanescent modes at the boundary of two
 333 isothermal media with different temperatures, that the evanescent regions are different in the upper
 334 and lower half-planes. On the (ω, k_x) plane, these regions are shifted relative to each other the
 335 more, the more is the value of d . At the same time, the wave modes at the interface of the media
 336 should remain evanescent in both media, and their dispersions should be enclosed within the overlap
 337 region of two evanescent regions. The cut-off curves for evanescent regions in the media under
 338 consideration are obtained in case of the null expressions under the radicals in (27) and (28). Gaps
 339 on the $\omega = f(k_x)$ dispersion curves are due to the evanescent areas of the two media do not match
 340 (see. Fig. 3).

341 Note that the dispersion curves $\omega = f(k_x)$ for values $d \leq 4$ are mostly inside both evanescent
 342 regions (see Fig. 3a, 3b), except for the longest waves. When $d \geq 4$, the dispersion curve $\omega = f(k_x)$
 343 breaks into two separate branches (see Fig. 3 c , 3 d). The long-wave branch is acoustic, and another
 344 branch with $k_x \geq 0.4H_1$ is surface gravity by its physical nature.

345

346 **6 Characteristic scales of ND and AE evanescent modes on the discontinuity**

347

348 In an unlimited isothermal medium, evanescent modes are separate “pure” solutions of
 349 hydrodynamic equations. At the interface between two isothermal media with different
 350 temperatures, dispersion of the evanescent modes have a combined character, composing different
 351 types of “pure” modes, depending on the value of the parameter d and spectral properties $\omega(k_x)$.

352 For some values of d , the curves of the dispersion equation (30) approach fairly close to the
 353 curves $\omega^2 = k_x g$ and $\omega^2 = k_x g(\gamma - 1)$, and also intersect them at different points. These intersection
 354 points correspond to the specific value of k_x , at which the dispersions of the ND and AE modes are
 355 realized, in the model under consideration, in a “pure” form. Let us now examine these cases in
 356 more detail. For this purpose, we substitute the dispersion relations $\omega^2 = k_x g$ and $\omega^2 = k_x g(\gamma - 1)$
 357 directly into (27), (28), and then into the boundary condition (30).

358 As was shown in Section 2, for dispersion relations $\omega^2 = k_x g$ and $\omega^2 = k_x g(\gamma - 1)$, values a_1
 359 and a_2 coincide and are determined by expressions (11). Consider the valid values of a_1 and a_2 for
 360 these dispersions with regard to the requirement of energy decay in both directions from the
 361 interface $a_1 > 1/2H_1$ and $a_2 < 1/2H_2$.

362

363 **6.1 Dispersion of the form $\omega^2 = k_x g$**

364

365 For a dispersion of the form $\omega^2 = k_x g$, we first analyze the stratification of the ND mode with
 366 $a_1 = k_x$, $a_2 = k_x$. In order for the energy of this mode to decay in both directions from the
 367 discontinuity, the following inequalities $1/2H_1 < k_x < 1/2H_2$ must be satisfied, i.e., $H_1 > H_2$.
 368 Therefore, ND mode can be realized at the discontinuity, if the ambient temperature in the upper

369 region is less and the density is greater than they are in the lower region. This situation corresponds
 370 to the unstable state of the atmosphere (see Roberts, B., 1991).

371 Take the stratification of the NDp modes in the form of $a_1 = \frac{1}{H_1} - k_x$, $a_2 = \frac{1}{H_2} - k_x$. The
 372 energy in this case decreases both ways from the discontinuity, if $1/2H_2 < k_x < 1/2H_1$, i.e. when
 373 $H_2 > H_1$. This condition corresponds to the stable state and the case under consideration. For the
 374 NDp mode from the dispersion equation (30) we get:

$$375 \quad H_2 \left(\frac{1}{\gamma H_2} - k_x \right) \left(2k_x - \frac{1}{H_1} \right) = H_1 \left(\frac{1}{\gamma H_1} - k_x \right) \left(2k_x - \frac{1}{H_2} \right), \quad k_x \neq 1/\gamma H_1, \quad k_x \neq 1/\gamma H_2. \quad (34)$$

376 From (34) it follows:

$$377 \quad k_x = \frac{d+1}{4dH_1} \left(1 \pm \sqrt{1 - \frac{8d}{\gamma(d^2-1)}} \right). \quad (35)$$

378 Figure 4a shows values of k_x for which the dispersion curve $\omega^2 = k_x g$ intersects with the
 379 calculated dispersion curve $\omega = f(k_x)$ depending on the parameter d . The upper solid curve in
 380 this figure corresponds to the solution (35) with the sign “+” before the radical and shows the points
 381 of intersection with the shorter wavelength branch. The lower dashed curve corresponds to the
 382 solution with a sign “-” and represents the points of intersection with the long-wavelength branch.
 383 For the upper curve $k_x \rightarrow 1/2H_1$ when $d \rightarrow \infty$. For $d < 2.5$, there are no intersections of the
 384 curve $\omega = f(k_x)$ calculated numerically from (30) with the curve for the dispersion $\omega^2 = k_x g$.

385 When combining the stratifications for ND modes as $a_1 = k_x$ and for NDp modes as
 386 $a_2 = \frac{1}{H_2} - k_x$, equation (30) yields the only possible value of $k_x = 1/2H_2$. For a combination of
 387 stratifications $a_1 = \frac{1}{H_1} - k_x$ (NDp), $a_2 = k_x$ (ND) we get $k_x = 1/2H_1$. Both of these cases do not
 388 satisfy the condition of energy decrease with height.

389 Thus, consideration of the possible values of a_1 and a_2 leads to the conclusion that on the
 390 interface of two isothermal media with $H_2 > H_1$ can only be implemented NDp mode with a
 391 dispersion $\omega^2 = k_x g$ and a specific scale $k_x \sim 1/2H_1$.

392
 393

394 **6.2 Dispersion of the form $\omega^2 = k_x g(\gamma - 1)$**

395

396 For the AE stratification of the form $a_1 = \frac{1}{H_1} - k_x$, $a_2 = \frac{1}{H_2} - k_x$ and for the AEp stratification of
 397 the form $a_1 = k_x$, $a_2 = k_x$, from the dispersion equation (30) follows the identity $H_1 = H_2$.
 398 Therefore, such modes do not realize at a temperature discontinuity. Apparently, to study the
 399 conditions of realization of AE and AEp modes, it is necessary to consider atmospheric models in
 400 which height profile $H(z)$ is continuous.

401 It should be noted that for the dispersion of the form $\omega^2 = k_x g(\gamma - 1)$, cases of combined modes
 402 stratifications are possible, satisfying the condition of decreasing energy on both sides of the
 403 boundary. So, for the combination of stratifications $a_1 = k_x$ (AEp), $a_2 = \frac{1}{H_2} - k_x$ (AE) from (30)
 404 we obtain the relation:

405
$$H_2 k_x (2 - \gamma) = H_1 \gamma \left(k_x - \frac{\gamma - 1}{\gamma H_1} \right).$$

406 Whence $k_x = \frac{\gamma - 1}{H_1 [\gamma - (2 - \gamma)d]}$. In this case, the inequality $d < \gamma / (2 - \gamma)$ must be satisfied. When
 407 $\gamma = 5/3$ we get the following restriction: $d < 5$. Given this limitation and condition $k_x > 1/2dH_1$,
 408 we obtain that a mode with a dispersion of $\omega^2 = k_x g(\gamma - 1)$ and stratification of AE type for the
 409 upper half-space and of AEp type for the lower half-space can propagate at the boundary in the
 410 range $1 < d < 5$ and for $k_x > 1/2H_1$. For the stratifications $a_1 = \frac{1}{H_1} - k_x$ (AE), $a_2 = k_x$ (AEp) from
 411 equation (30) we obtain the relation:

412
$$H_2 \gamma \left(k_x - \frac{\gamma - 1}{\gamma H_2} \right) = H_1 k_x (2 - \gamma).$$

413 It implies the ratio $k_x = \frac{\gamma - 1}{H_1 [\gamma d - (2 - \gamma)]}$, in which the parameter d can take any values with $d > 1$,
 414 and the horizontal wave number is limited by the inequality $k_x < 1/2H_1$. Features of the behavior of
 415 the $\omega^2 = k_x g(\gamma - 1)$ mode at the discontinuity, depending on the scale k_x are shown in Fig. 4b.

416

417 7 Discussion

418

419 Let us dwell on some of the results in terms of their use for the analysis of experimental data.

420 With the f -mode observed on the Sun, one should identify the mode that we classify as ND
421 mode, for which $\omega^2 = k_x g$, $V_z \sim \exp(k_x z)$ and $\text{div}\vec{V} = 0$ (Roberts, B., 1991). In the framework of
422 the considered temperature discontinuity model, it was shown that with $T_1 < T_2$ (corresponds to the
423 chromosphere-corona interface) the condition for decreasing amplitude with height to both sides of
424 the interface is satisfied only by the NDp mode with $\omega^2 = k_x g$, $V_z \sim \exp\left(\frac{1}{H} - k_x\right)z$ and $\text{div}\vec{V} \neq 0$.

425 When the ratio $d \rightarrow \infty$ (i.e., $H_2/H_1 \rightarrow \infty$), the NDp mode with $k_x \rightarrow 1/2H_1$ asymptotically
426 approaches ND mode. On the interface between the chromosphere and the solar corona d is large,
427 but of finite magnitude: $d \sim 50$ (Athay, 1976; Jones, 1969). Therefore, the condition of the
428 presence of a free surface, which is required for the realization of the ND mode, is fulfilled only
429 approximately. Therefore, in the framework of the temperature discontinuity model, the f -mode
430 observed on the Sun should not be associated with the non-divergent ND mode, but with non-
431 divergent *pseudo* – mode NDp.

432 For the Earth's atmosphere, the maximum possible value of d is observed at the interface
433 between the thermosphere with $T_2 \sim 800 - 1500K$ (depending on solar activity) and the underlying
434 atmosphere with $T_1 \sim 300K$. When $d = 5$, the dispersion (30) asymptotically tends
435 to $\omega^2 = k_x g(\gamma - 1)$ with $k_x \rightarrow \infty$. Therefore, it can be expected that evanescent modes in this case
436 will be close to $\omega^2 = k_x g(\gamma - 1)$.

437 In other layers of the earth's atmosphere we have $d \leq 1.3$ (Jursa, 1985). As follows from (33),
438 for small values of $d \leq 1.3$ and for the wavelengths in the interval $k_x \sim (0.5 - 1.5)H_1$, the relation
439 $\omega^2 \rightarrow N^2$ is satisfied (see Fig. 2). Therefore, it can be expected that at small positive temperature
440 gradients in the atmosphere, waves with a frequency close to the frequency of Brent-Väisälä should
441 prevail. These conclusions experimentally confirm (Shimkhada et al., 2009) the results of
442 observations of short-period evanescent waves with small wavelengths at altitudes near the
443 mesopause.

444

445 8 Main results

446

447 In the paper, different types of evanescent acoustic-gravity modes characteristic of an isothermal
448 atmosphere are investigated. A new mode was derived in the form of anelastic acoustic-gravity
449 wave mode with the dispersion equation $\omega^2 = k_x g (\gamma - 1)$. The main properties of the AE mode
450 are presented in Table 1 in comparison with other known evanescent modes. It is shown that for
451 both anelastic and non-divergent modes there are pseudo-modes that satisfy the same dispersions,
452 but having different polarization and the dependence of the amplitude of the disturbances on the
453 height.

454 For AE and ND evanescent modes, the value of $k_x \rightarrow 1/2H$ sets a special scale (wavelength) at
455 which these modes are identical to their pseudo-modes AEp and NDp. In addition, at the same point
456 they are adjacent to the boundaries of the continuous spectrum (AE mode to the gravity region, and
457 ND mode to the acoustic region, respectively).

458 The features of the evanescent modes realization at the interface of two isothermal media are
459 considered. It is shown that in this case, dispersions of evanescent modes are combined, merging
460 the features of different types of modes characteristic of an unbounded isothermal atmosphere. This
461 effect is most pronounced in the following asymptotic cases: 1) when $d \rightarrow \infty$, we obtain the
462 dispersion for the ND (NDp) mode in the form $\omega^2 \approx k_x g$; 2) when $d \rightarrow 1$, for scales $k_x \sim H_1$, a
463 mode with $\omega^2 \approx N_1^2$ is realized; 3) for $k_x \rightarrow 0$, a Lamb wave with a dispersion relation of the form
464 $\omega^2 \approx c_2^2 k_x^2$ is obtained, which depends only on the parameters of the medium in the upper half-
465 space.

466 It was demonstrated that on the interface of two isothermal media with $T_2 > T_1$, the NDp mode
467 with the dispersion $\omega^2 = k_x g$ and the selected scale $k_x \sim 1/2H_1$ is realized. At the same time, the
468 ND mode does not satisfy the condition of decreasing energy on each side of the interface.
469 Dispersion $\omega^2 = k_x g (\gamma - 1)$ on the interface of two media is satisfied by the wave mode, which
470 has different types of amplitude versus height dependencies at different horizontal scales k_x . When
471 $k_x > 1/2H_1$, the height dependence of AE amplitude for $z > 0$ and AEp amplitude for $z < 0$ satisfy
472 the condition of decreasing energy from the interface. On the contrary, when $k_x < 1/2H_1$, this
473 condition is satisfied by AEp amplitude for $z > 0$ and AE amplitude for $z < 0$.

474 It is important to note that according to our analysis in the framework of the temperature
475 discontinuity model: (1) the f - mode observed on the Sun should not be associated with the non-

476 divergent ($\omega^2 = k_x g, \text{div}V = 0$) mode, but with its non-divergent *pseudo*-mode ($\omega^2 = k_x g,$
477 $\text{div}V \neq 0$). (2) At the interface between the earth's thermosphere and the underlying atmosphere it
478 can be expected that evanescent modes with short wavelengths will be close to the new mode
479 ($\omega^2 = k_x g(\gamma - 1)$). (3) Oscillations with a frequency close to the frequency of Brent-Väisälä should
480 prevail at altitudes near the earth's mesopause.

481 *Acknowledgements.* This publication is based on work supported in part by Integrated Scientific
482 Programmes of the National Academy of Science of Ukraine on Space Research and Plasma
483 Physics.

484

485 **References**

486

487 Antia, H.M.: Estimate of solar radius from f-mode, *Astron. Astrophys.*, 330, 336-340, 1998.

488 Athay, R.G.: *The Solar Chromosphere and Corona: Quiet Sun.* Dordrecht, Holland: Reidel, 504,
489 1976.

490 Beer, T.: *Atmospheric Waves,* John Wiley, New York, 300 pp, 1974.

491 Belashov, V.Yu.: Dynamics of nonlinear internal gravity waves at ionosphere F-region heights,
492 *Geomagn. Aeron. (Engl. Transl.)*, 1990. 30, 637-641, 1990.

493 Bannon, P.R.: On the anelastic approximation for a compressible atmosphere, *J. Atmos. Sci.*, 53, 23,
494 3618 – 3628, 1996.

495 Cheremnykh, O., Cheremnykh, S., Kozak, L., Kronberg, E.: Magnetohydrodynamics waves and the
496 Kelvin_Helmholtz instability at the boundary of plasma mediums, *Phys. Plasmas*, 25, 10, 102119,
497 2018a.

498 Cheremnykh, O.K., Fedun, V., Ladikov-Roey, Y.P., Verth, G.: On the stability of incompressible
499 MHD modes in magnetic cylinder with twisted magnetic field and flow, *Astrophys. Journ.*, 866, 2,
500 86, 2018b.

501 Cheremnykh, O.K., Selivanov, Yu.A., Zakharov, I.V.: The influence of compressibility and non-
502 isothermality of the atmosphere on the propagation of acoustic-gravity waves, *Kosm. nauka tehnol.*,
503 16, 1, 09–19, doi.org/10.15407/knit2010.01.009, 2010.

504 Fedorenko, A.K.: Energy Balance of Acoustic Gravity Waves above the Polar Caps According to
505 the Data of Satellite Measurements, *Geomagn. Aeron.* 50, 107–118, 2010.

506 Fedorenko, A.K., Kryuchkov, Y.I.: Wind Control of the Propagation of Acoustic Gravity Waves in
507 the Polar Atmosphere, *Geomagn. Aeron. (Engl. Transl.)* 53, 377-388, 2013.

508 Fedorenko, A.K., Bespalova, A.V, Cheremnykh, O.K, Kryuchkov, E.I.: A dominant acoustic-gravity
509 mode in the polar thermosphere, *Ann. Geophys.*, 33, 101-108, 2015. [doi:10.5194/angeo-33-101-
510 2015].

511 Fedorenko, A.K., Kryuchkov, E.I., Cheremnykh, O.K., Klymenko, Yu.O., Yampolski Yu.M.:
512 Peculiarities of acoustic-gravity waves in inhomogeneous flows of the polar thermosphere, *J.*
513 *Atmos. Solar-Ter. Phys.*, 178, 17-23, 2018. doi.org/10.1016/j.jastp.2018.05.009

514 Francis, S.H.: Global propagation of atmospheric gravity waves: A review, *J. Atmos.Terr. Phys.*, 37,
515 1011-1054, 1975.

516 Ghosh, P., Antia, H.M., Chitre, S.M.: Seismology of the solar f-mode. I. Basic signatures of
517 shearing velocity fields, *Astrophys. J.*, 451, 851-858, 1995.

518 Hines, C.O.: Internal gravity waves at ionospheric heights, *Can. J. Phys.*, 38, 1441–1481, 1960.

519 Huang, K.M., Zhang, S.D., Yi, F., Huang, C.M., Gan, Q., Gong, Y., Zhang, Y. H.: Nonlinear
520 interaction of gravity waves in a nonisothermal and dissipative atmosphere, *Ann. Geophys.*, 32, 263-
521 275, 2014. [doi:10.5194/angeo-32-263-2014].

522 Innis, J.L., Conde, M.: Characterization of acoustic-gravity waves in the upper thermosphere using
523 Dynamics Explorer 2 Wind and Temperature Spectrometer (WATS) and Neutral Atmosphere
524 Composition Spectrometer (NACS) data, *J. Geophys. Res.*, 107, NoA12, 2002. [doi: 10.1029/2002
525 JA009370].

526 Johnson, F.S., Hanson, W.B., Hodges, R.R., Coley, W.R., Carignan, G.R., Spencer, N.W.: Gravity
527 waves near 300 km over the polar caps, *J. Geophys. Res.*, 100, 23993-24002, 1995.

528 Jones, Walter L.: Non-divergent oscillations in the Solar Atmosphere, *Solar Phys.*, 7, 204-209, 1969.

529 Jursa, Adolph S.: Handbook of geophysics and the space environment. Vol. 1. Hanscom Air Force
530 Base, MA: Air Force Geophysics Laboratory, Air Force Systems Command, United States Air
531 Force, 1040, 1985.

532 Kaladze, T.D., Pokhotelov, O.A., Shah, H.A., Khan, M.I., Stenflo, L.: Acoustic-gravity waves in the
533 Earth's ionosphere, *J. Atmos. Solar-Terr. Phys.*, 70, 1607–1616, 2008.

534 Ladikov-Roev, Y.P., Cheremnykh, O.K.: *Mathematical Models of Continuous Media*, Naukova
535 Dumka, Kyiv, 552, 2010 (in Russian).

536 Miles, Alan, J., Roberts, B.: Magnetoacoustic-gravity surface waves. I. Constant Alfvén Speed,
537 *Solar Phys.*, 141, 205-234, 1992.

538 Nekrasov, A.K., Shalimov, S.L., Shukla, P.K., Stenflo, L.: Nonlinear disturbances in the ionosphere
539 due to acoustic gravity waves, *J. Atmos. Terr. Phys.*, 57, 732–742, 1995.

540 Roberts, B.: MHD Waves in the Sun, in: *Advances in solar system magnetohydrodynamics*, CUP,
541 239, 1991.

542 Rosental, C.S., Gough, D.O.: The Solar f-mode as interfacial mode at the chromosphere-corona
543 transition. *The Astrophysical Journal*, 423, 488-495, 1994.

544 Simkhada, D.B., Snively, J.B., Taylor, M.J., Franke, S.J.: Analysis and modeling of ducted and
545 evanescent gravity waves observed in the Hawaiian airglow. *Ann. Geophys.* 27, 3213-3224, 2009.

546 Stenflo, L., Shukla, P. K.: Nonlinear acoustic-gravity waves, *J. Plasma Phys.*, 75, 841–847, 2009.
547 [doi.org/10.1017/S0022377809007892].

548 Tolstoy, I.: The theory of waves in stratified fluids including the effects of gravity and rotation, *Rev.*
549 *of Modern Phys.*, Vol. 35, N1, 1963.

550 Vadas, S. L., Nicolls, M. J.: The phases and amplitudes of gravity waves propagating and
551 dissipating in the thermosphere: Theory, *J. Geophys. Res.*, 117, A05322,
552 [doi:10.1029/2011JA017426](https://doi.org/10.1029/2011JA017426), 2012.

553 Waltercheid, R.L., Hecht, J.H.: A reexamination of evanescent acoustic-gravity waves: Special
554 properties and aeronomical significance, *J. Geophys. Res.*, 108, D11, 4340,
555 [doi:10.1029/2002JD002421](https://doi.org/10.1029/2002JD002421), 2003.

556 Yeh, K.S., Liu, C.H.: Acoustic-gravity waves in the upper atmosphere, *Rev. Geophys. Space. Phys.*,
557 12, 193-216, 1974.

558

559

560 Table 1. Properties of different evanescent acoustic-gravity modes

Mode type	Dispersion	a	Polarization
Lamb Wave (L)	$\omega^2 = k_x^2 c^2$	$\frac{\gamma - 1}{\gamma H}$	$V_z = 0; V_x \neq 0$
Lamb's Pseudo-mode (Lp)		$\frac{1}{\gamma H}$	$V_x(2 - \gamma)k_x g = i(N^2 - k_x^2 c^2)V_z$
BV Oscillations (BV)	$\omega^2 = N^2$	$\frac{1}{\gamma H}$	$V_x = 0; V_z \neq 0$
BV Pseudo-mode (BVp)		$\frac{\gamma - 1}{\gamma H}$	$V_x(k_x^2 c^2 - N^2) = i(2 - \gamma)k_x g V_z$
Non-divergent (ND) mode, $div \vec{V} = 0$	$\omega^2 = k_x g$	k_x	$V_x = -iV_z$
Pseudo-non-divergent mode (NDp), $div \vec{V} \neq 0$		$\frac{1}{H} - k_x$	$V_x \left(\frac{1}{\gamma H} - k_x \right) = -i \left(k_x - \frac{\gamma - 1}{\gamma H} \right) V_z$
Anelastic mode (AE), $div(\rho_0 \vec{V}) = 0$	$\omega^2 = k_x g(\gamma - 1)$	$\frac{1}{H} - k_x$	$V_x = iV_z$
Pseudo-anelastic mode (AEp), $div(\rho_0 \vec{V}) \neq 0$		k_x	$V_x \left(k_x - \frac{\gamma - 1}{\gamma H} \right) = i \left(\frac{1}{\gamma H} - k_x \right) V_z$

561

562

563 Table 2. The coincidence of the evanescent mode properties at the intersection points of the
 564 dispersion curves *

Lamb Wave (L)	Lamb's Pseudo-mode (Lp)	BV Oscillations (Bv)	BV Pseudo-mode (Bvp)	Non-divergent mode (ND)	Pseudo-non-divergent mode (NDp)	Anelastic mode (AE)	Pseudo-anelastic mode (AEp)
BVp NDp AEp	BV ND AE	Lp NDp AEp	L ND AE	Lp BVp	L BV	Lp BVp	L BV

565

566 * *Note.* The bottom rows show the modes that are indistinguishable from the corresponding
 567 mode of the top row at the point of intersection of the dispersion curves.

568

569

Table 3. The change in energy density of evanescent modes with height in an infinite isothermal

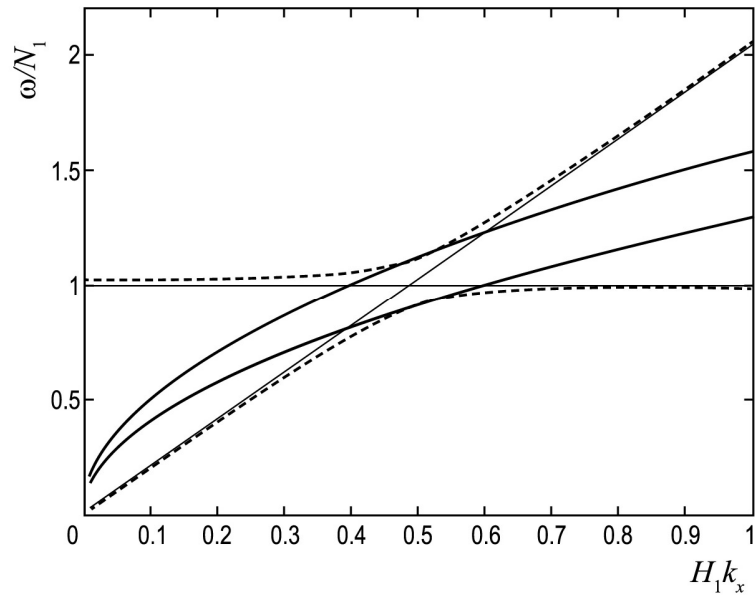
570

atmosphere

Domain	Lamb Wave (L)	Lamb's Pseudo-mode	BV Oscillations (BV)	BV Pseudo-mode	Non-divergent mode (ND)	Pseudo-non-divergent mode (NDp)	Anelastic mode (AE)	Pseudo-anelastic mode (AEp)
$z \rightarrow +\infty$	$E \rightarrow 0$	$E \rightarrow \infty$	$E \rightarrow \infty$	$E \rightarrow 0$	$E \rightarrow 0,$ $k_x < 1/2H$ $E \rightarrow \infty,$ $k_x > 1/2H$	$E \rightarrow 0,$ $k_x > 1/2H$ $E \rightarrow \infty,$ $k_x < 1/2H$	$E \rightarrow 0,$ $k_x > 1/2H$ $E \rightarrow \infty,$ $k_x < 1/2H$	$E \rightarrow 0,$ $k_x < 1/2H$ $E \rightarrow \infty,$ $k_x > 1/2H$
$z \rightarrow -\infty$	$E \rightarrow \infty$	$E \rightarrow 0$	$E \rightarrow 0$	$E \rightarrow \infty$	$E \rightarrow \infty,$ $k_x < 1/2H$ $E \rightarrow 0,$ $k_x > 1/2H$	$E \rightarrow \infty,$ $k_x > 1/2H$ $E \rightarrow 0,$ $k_x < 1/2H$	$E \rightarrow \infty,$ $k_x > 1/2H$ $E \rightarrow 0,$ $k_x < 1/2H$	$E \rightarrow \infty,$ $k_x < 1/2H$ $E \rightarrow 0,$ $k_x > 1/2H$

571

572



573

574

575

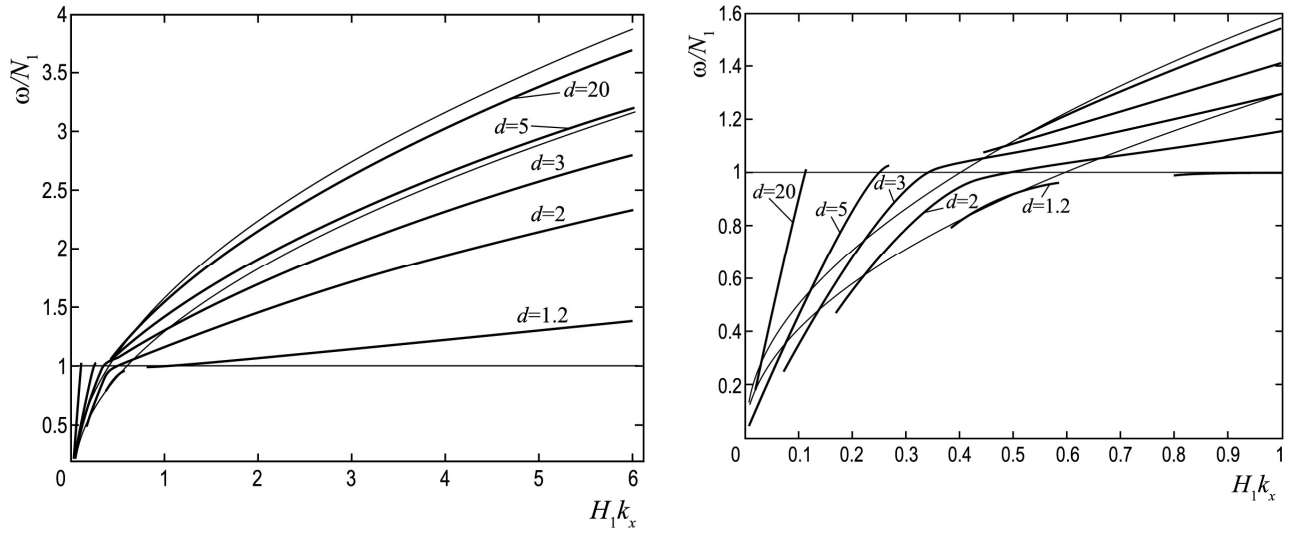
576

577

578

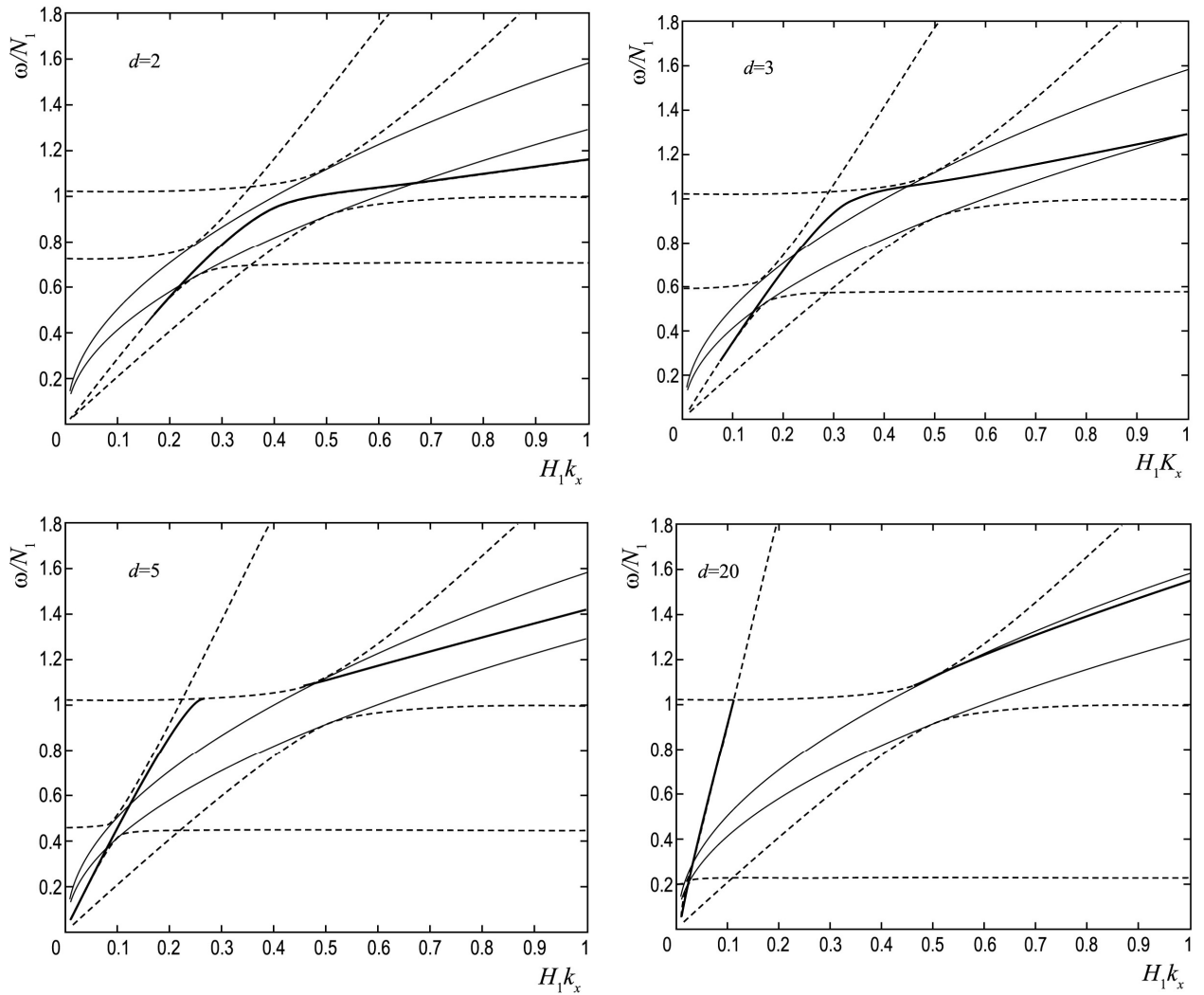
Fig. 1. Dispersion dependencies $\omega = f(k_x)$: 1) boundaries between acoustic and gravity regions for freely propagating waves (dashed lines); 2) evanescent mode: $\omega = \sqrt{k_x g}$ (upper solid curve) and $\omega = \sqrt{k_x g(\gamma - 1)}$ (lower solid curve), $\omega = N$ (thin horizontal line), $\omega = k_x c$ (thin sloping straight line).

579



580
 581
 582
 583
 584
 585

Fig. 2. Dispersion dependencies $\omega = f(k_x)$ at the boundary of the discontinuity for different values of the parameter d . General dependence (a), long-wave part in more detail (b). Thin curves denote $\omega = \sqrt{k_x g}$ (upper curve) and $\omega = \sqrt{k_x g(\gamma - 1)}$ (lower curve), $\omega = N$ (horizontal line)



587

588

589

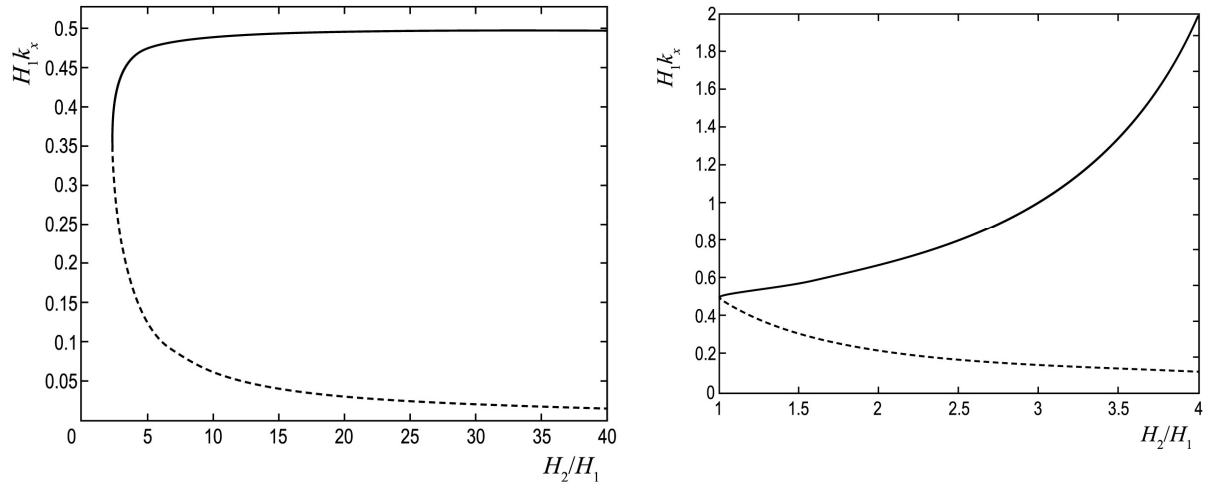
590

591

592

Fig. 3. Dispersion dependencies of the $\omega = f(k_x)$ type at the temperature discontinuity boundary for $d = 2$ (a), $d = 3$ (b), $d = 5$ (c), $d = 20$ (d). The dashed curves represent the boundaries of the areas with free propagation of AGW in the upper and lower half-space. Thin curves denote $\omega = \sqrt{k_x g}$ (upper curve) and $\omega = \sqrt{k_x g(\gamma - 1)}$ (lower curve).

593



594

595

596

597

598

Fig. 4. Horizontal scales $k_x H_1$, on which the modes with the dispersion $\omega^2 = k_x g$ (a) and $\omega^2 = k_x g(\gamma - 1)$ (b) are realized, depending on $d = H_2 / H_1$.